Complexity analysis of heartbeat-related signals in Brain MRI time series as a potential biomarker for ageing and cognitive performance

David López Pérez[a,b], Arun L.W. Bokde[c] & Christian Kerskens[b]

[a]Institute of Psychology, Polish Academy of Sciences, Warsaw, Poland

[b]Institute of Neuroscience, Trinity College, Dublin, Ireland

[c]Trinity College Institute of Neuroscience and Cognitive Systems Group, Discipline of Psychiatry, School of Medicine, Trinity College Dublin, Ireland

* Correspondence:

David López Pérez, d.lopez@psych.pan.pl, Institute of Psychology, Polish Academy of Sciences, Jaracza, 1, 00-378 Warsaw, Poland, tel. 0048 666331709

Acknowledgements

We would like to thank Elizabeth G. Kehoe and Dervla Farrell for assistance in acquiring the data, the Trinity College's IT Research, Sojo Joseph for carrying out the imaging protocols for all participants and Edyta Stanaszek for reading earlier versions of the manuscript. This work was supported by Science Foundation Ireland (SFI-11/RFP.1/NES/3051), the Science Foundation Ireland Stokes Programme (07/SK/B1214a), from the European Regional Development Fund via the Interregional 4A Ireland Wales Programme 2007–2013 and Trinity College Institute of Neuroscience. This project has received additional funding from the Institute of Psychology, Polish Academy of Sciences.

Abstract

There are multiple magnet resonance imaging (MRI) based approaches to studying the ageing brain. Getting older affects both the structure of the brain and our cognitive capabilities, but there is still no solid evidence on how ageing influences the mechanisms underlying the MRI signal. Here, we apply a zero-spin echoes (ZSEs) weighted MRI sequence which recently was found to be sensitive to wakefulness. We investigated the complexity of the signal time series of this sequence in two age groups; young (18-29 years) and old (over 65 years). While comparing young and old participants, we found qualitative and quantitative evidence that the dynamics of ZSE fluctuations undergo strong changes with age. Finally, we study how differences in complexity of the ZSE signal relate with measures from different cognitive batteries, suggesting that ZSE may reveal cognitive functioning in a new. fashion. The profound sensitivity for dynamic changes shows the potential of ZSE and its underlying physiological mechanism with clinical relevance for all neurovascular diseases.

Keywords: Complexity, Quantum Coherence, Cognitive Ageing, MRI, Consciousness

Introduction

It is well established that normal ageing has cascading effects on many cognitive domains and affects the brain at multiples levels ranging from sub- to macro-cellular (e.g., Salat et al., 2004; Allen et al., 2005). For instance, older adults have particular difficulties with episodic memory (Craik & Bosman, 1992), working memory (e.g., Balota, Dolan, & Duchek, 2000) or are slower processing different stimuli (e.g., Salthouse, 1996). At the same time, some aspects of cognition are maintained, such as semantic memory (Laver, 2009) or emotional regulation (Carstensen, 2011). However, the cerebral mechanisms that underlie this better or lesser performance are still poorly understood (Grady, 2012). A vast number of studies have tried to link these structural changes to age differences in cognitive function. Magnetic resonance imaging (MRI) based methods have been mainly used to study changes in the ageing brain. Among the various MRI methods, functional MRI (fMRI), with more than 10000 published papers, is probably the one more widely applied (e.g., Tsvetanov, Henson, & Rowe, 2019). The blood oxygen level-dependent (BOLD) signal obtained from fMRI is an indirect index of neural activity and reflects small metabolic changes in deoxyhaemoglobin concentrations that take place when a specific region of the brain is active (Ogawa et al., 1990). These responses have been found to be similar in both young and older adults (Grady, 2012), but in some cases, the magnitude of the BOLD response was reduced in older adults (e.g., Archer et al., 2018) while sometimes was increased (e.g., Liu et al., 2013). The former is often related to cognitive deficits in older adults (e.g., Grady et al., 1995), while the latter is often interpreted as compensatory (e.g., Grady et al., 1994) or as a reduction in the selectivity of responses (Grady, 2008). Independently of the direction of these magnitude variations, changes in cerebral vasculature with age (e.g., Goyal et al., 2016), are somehow expected to influence the mechanisms underlying the fMRI signal. Although still unknown, these changes should be related to differences in cognitive performance, but no substantial evidence has been found so far.

This comes as a surprise because heart functions also alter with age which should, in turn, affect cerebral blood flow. Even more, it is well known that several heartbeat-related effects influence conscious perception where the cardiac cycle may impact the perception of visual or auditory stimuli (e.g., Al et al., 2020). The existence of heartbeat-evoked potential (HEP) in general is strong evidence that the heartbeat influences neuronal functions (Montoya, Schandry, & Müller, 1993). In a recent study, López Pérez and Kerskens (2019) discovered zero-spin echoes (ZSEs) in fast MRI time series which were evoked by the blood pulsation. Surprisingly, they found those signals only if the volunteers were awake which suggest that they have found another measure like the HEPs that relates heartbeat with conscious perceptions. The contrast mechanism of ZSEs is usually based on long-range zero quantum coherence (ZQC) or similar quantum effects which has not traditionally been considered as a powerful tuning element for enhancing or explaining functions in biology (Scholes et al., 2017). However, a growing body of literature has recently demonstrated that quantum coherence in living organisms exists and it is itself essential for their functioning (e.g., Engel et al., 2007; Huelga & Plenio, 2013). With the recent rise of the field of quantum biology, it has been suggested that quantum phenomena might also influence brain activity and affect its cognition (Jedlicka, 2017). Although, the ZSE signals were robust and reliable (López Pérez & Kerskens, 2019), it showed a high variability and complexity, which suggest that the interaction between the brain and the heart would be high-dimensional, and thus, the complexity of the system (i.e., its ability to adapt and function in an ever-changing environment) would also be high-dimensional (Jedlicka, 2017; Peng, Costa, & Goldberger, 2009). Recent studies have shown that high complexity is characteristic to healthy systems and that can degrade because of disease or ageing (Dos Santos et al., 2014). Thus, if this mechanism is vital for cerebral dynamics, the complexity of these fluctuations needs to be kept high and any variation on the dynamics with age should affect the complexity of the system.

In this paper, we want to study, for the first time, how the dynamical complexity of the long-range quantum coherence signal may vary with age. To characterise these fluctuations as

117 entirely as possible, we use a broad range of dynamical systems measures. First, we applied
118 Recurrence Quantification Analysis (RQA; Zbilut & Webber, 1992), which is an increasingly
119 popular method to analyse dynamical changes of behaviour in complex systems. This concept has
120 been used to study physiological signals (Marwan & Webber, 2015; Wessel et al., 2003) heart rate
121 variability (Dos Santos et al., 2014) or the dynamics of heart rhythm modulation (Censi,
122 Calcagnini, & Cerutti; 2015). The main benefits of RQA in comparison to standard analysis resides
123 in its sensitivity to small changes in the system dynamics (Dos Santos et al., 2014). Secondly, we
124 employed MultiFractal Detrended Fluctuation Analysis to extract the fractal properties of the
125 signal (MFDFA; Ihlen, 2012). Multifractal Analysis is another efficient chaos theory method to
126 study the fractal scaling properties and long-range correlations of noisy signals (Peng et al., 2009;
127 for a review see Lopes & Betrouni, 2009). Fractal differences as a consequence of ageing have
128 been found between monofractal or multifractal signals in EEG (Pereda et al., 1998) or due to
129 HRV changes (Makowiec et al., 2011). Finally, we relate these measures with different cognitive
130 batteries and show that those quantum fluctuations may be key for cerebral dynamics and cognitive
131 functioning.

132 **Methods**

133 ***Participants***

134 60 subjects (29 participants between 18 and 29 years old, and 31 participants over 65 years
135 old) were scanned with the protocols approved by the St. James Hospital and the Adelaide and
136 Meath Hospital, incorporating the National Children Hospital Research Ethics Committee. All
137 participants were adults recruited for a larger study (Kehoe et al., 2015; Alderson et al., 2017;
138 Gilligan et al., 2019) and came from the greater Dublin area.

139 All participants underwent the Cambridge Neuropsychological Test Automated Battery
140 (CANTAB; Robbins et al., 1994) which has been used to detect changes in neuropsychological
141 performance and include tests of working memory, learning and executive function; visual, verbal

and episodic memory; attention, information processing and reaction time; social and emotion recognition, decision making and response control. The CANTAB scores were normalised for age and IQ. Particularly, the following subtest were administered:

- The Paired Associate Learning Test is a measure of episodic memory where boxes are displayed on the screen, and each one has a distinct pattern. The boxes are opened in random order, revealing the pattern behind the box. In the test phase, patterns are individually displayed in the centre of the screen, and participants must press the box that shields the respective pattern.

- Pattern Recognition Memory is a test of visual pattern recognition memory in which the participant is presented with a series of visual patterns, one at a time, in the centre of the screen. In the recognition phase, the participant is required to choose between a pattern they have already seen and a novel pattern. In this phase, the test patterns are presented in the reverse order to the original order of presentation. This is then repeated, with new patterns. The second recognition phase can be given either immediately (immediate recall) or after a delay (delay recall).

- The Spatial Working Memory Test assesses spatial working memory in which boxes are presented on the computer screen and hidden behind one of the boxes is a yellow circle. Participants must find the box where the yellow circle is located. As the task progresses, the number of boxes on the screen increases. We analysed the spatial working memory strategies (i.e., the number of times participants begin a new search strategy from the same box).

Moreover, participants performed the trail making test (TNT; Reitan, 1958) which is a neuropsychological test of visual attention and task switching. TNT test that can provide information about visual search speed, scanning, speed of processing, mental flexibility, as well as executive functioning (Arnett & Labovitz, 1995).

MRI data acquisition

Each participant was imaged in a 3.0 T Philips whole-body MRI scanner (Philips, The Netherlands) using a standard single-shot GE EPI sequence operating with a 8-channel array receiver coil in all cases. The parameters of the EPI time-series sequence were as follows: Flip angle = 30º, TR = 60 ms and the TE = 18 ms with a voxel size was 3.5 x 3.5 x 3.5 mm, matrix size was 64 x 64, SENSE factor 3, bandwidth readout direction was 2148 Hz and saturation pulse was 6 ms with 21 mT/m gradient strength. The imaging slice was set coronal above the ventricle to avoid pulsation effects (see Figure 1 for example). In addition, two saturation slices of 5 mm in thickness were placed parallel to the imaging slice (15 mm above and 20 mm below). These slabs were applied to introduce asymmetrical magnetic gradient scheme to generate ZSE (for a full description see López Pérez and Kerskens, 2019). Additional scans without the saturation slabs using the same imaging parameters were carried out which had two effects on the ZSE; a change of the angulation between the asymmetric gradient field and the main magnet field towards the magic angle (lowering the dipole-dipole coupling effect) and a lengthening of the ZQC correlation distance. As a result, ZSE were strongly reduced leaving only higher-order coherence in the time-series and very long-distance quantum coherence. In this manuscript, we refer to these scans as the single quantum coherence (SQC) weighted signal to differentiate it from the ones that contain higher amount of ZSE component (ZSE weighted signal). The average angulation of the imaging

slice was 14.76 ± 5.65 degrees and for each participant the angulation was always the same during the acquisition with the slab and without it.

Anatomical MRI images in all studies included a high-resolution sagittal, T1-weighted MP-RAGE (TR = 2.1 s, TE = 3.93 ms, flip angle = 7°). The ZSE-weighted sequence was acquired after the resting-state fMRI part of the session. The radiographer always contacted the participants before the acquisition to make sure that they were awake. This step is important given that the ZSE signal has been suggested to be sensitive to changes in wakefulness of the participant (López Pérez and Kerskens, 2019).

Signal Preprocessing

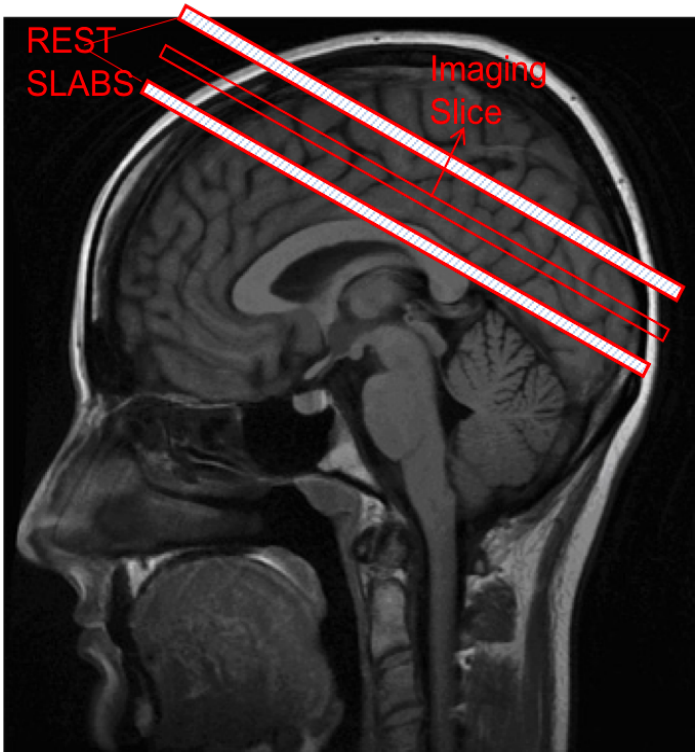

Figure 1. *Acquisition model which includes the image slice (central red line) and the REST slabs above and below the imaging slice both 5 mm thick and separated 15 mm and*

All calculations were developed in a Dell Optiplex 790 with 12 Gb RAM using Matlab 2017a (The MathWorks Inc., Natick, MA, 2017). Since motion correction could not be applied due to the single slice nature of the experiment, average time-series were visually inspected in

194 search for irregularities which were manually removed from the analysis leaving the rest of the
195 time-series unaltered. In addition, the data was not smoothed to avoid removing low frequencies
196 which may lead to the loss of information (Pignat et al., 2013). Manual segmentation was used to
197 create a mask to remove cerebrospinal fluid (CSF) contributions which were later eroded to avoid
198 partial volume effects at the edges. The first 100 scans were removed to avoid signal saturation
199 effects.

200 ***Recurrence Quantification Analysis***

201 We used Recurrence Quantification Analysis (RQA) to analyse the dynamical temporal
202 characteristics of the MRI signals. RQA quantifies the repeated occurrences of a given state of a
203 system (i.e., recurrences) by analysing the different structures present in a recurrence plot, which
204 is a graphical representation of the recurrences in the dynamical system (Zbilut & Webber, 1992).
205 In our analysis, we considered the following RQA measures (Bosl, Loddenkemper, & Nelson,
206 2017):

207 • Determinism (Det): it represents a measure that quantifies repeating patterns in a system
208 and it is a measure of its predictability. Regular, periodic signals, such as sine waves,have
209 higher DET values, while uncorrelated time-series cause low DET.

210 • Mean Line (MeanL): it is the average length of repeating patterns in the system. It
211 represents the mean prediction time of the signal, a measure of chaos or divergence from
212 an initial point.

213 • Entropy (Ent): it is the Shannon entropy of the distribution of the repeating patterns of
214 the system. If a signal has high entropy it exhibits diversity in short- and long-duration
215 periodicities.

- Laminarity (Lam): it determines the frequency of transitions from one state to another, without describing the length of these transition phases. It indexes the general level of persistence in some particular state of one of the time-series (Hirata & Aihara, 2010).

- Trapping Time (TT): it represents the average time the system remains on a given state and it is a measure of the stability of the system. It was calculated here using the *tt* function from the CRP Toolbox for Matlab (Marwan et al., 2002).

- Maximum Line (MaxL): it is the largest Lyapunov exponent of a chaotic signal, which gives the longest time spent in a single state by the system (Gómez & Hornero, 2010).

Three critical parameters need to be set to calculate the recurrence plots. First, the smallest sufficient embedding dimension was determined using the *fnn* function (Kennel, Brown & Abarnel, 1992) within the CRP Toolbox (Marwan, N.: Cross Recurrence Plot Toolbox; Marwan et al., 2007, for MATLAB, Ver. 5.22 (R31.2), http://tocsy.pik-potsdam.de/CRPtoolbox/). This function estimates the minimum embedding dimension where the false nearest neighbours vanish. We applied the *fnn* to all time-series and obtained an average value of 15, which agrees with the typical values recommended for biological signals (Marwan & Webber, 2015). The second parameter is the delay which we calculated using the mi function from the CRP Toolbox (Marwan et al., 2007; Roulston, 1999). This function finds the non-linear interrelations in the data and determines which delay fulfils the criterion of independence. In the same way as the embedding dimension, we applied the *mi* function to all time-series and we obtained an average value of 3. Finally, several criteria have been suggested for the choice of the recurrence threshold (Thiel et al., 2002). Here, we adapted the radius for each time-series using the embedding dimension and delay computed together with a recurrence rate sufficiently low (i.e., RR = 3%) (Marwan et al., 2002). Additional parameters in the RQA calculations were Euclidean normalisation for each time-series and minimum line length equal to 2.

Multifractal Detrended Fluctuation Analysis

In biological systems, the coupling between different systems often exhibits (Peng et al., 2009) different spatial and temporal scales and hence its complexity is also multi-scale and hierarchical (Peng et al., 2009). Thus, to analyse the scale-invariant properties of the MRI segments and its changes with age we used Multifractal Detrended Fluctuation Analysis (MFDFA). To do so, we first, calculated the multifractal spectrum, *D,* of each time-series using the MFDFA Matlab Toolbox (Ihlen, 2012). The multifractal spectrum identifies the deviations in fractal structure within time-periods with large and small fluctuations (Ihlen, 2012). Each spectrum was computed using a window length with a minimum value of 2 and a maximum value of half the length of the time-series. The *q*-order statistical moments were chosen between -11 and 11 and divided into 21 steps (see further description in Ihlen, 2012).

From each fractal spectrum, two parameters were calculated, i.e., the width of the spectrum *W* and the position of the spectrum maxima *H*. The width *W* is calculated by subtracting the lower part of the spectrum, *h*, to the upper part of the spectrum, h (Ihlen, 2012; Makowiec et al., 2011; Ma et al., 2006). A small width indicates that the time-series has fewer singularities and tends to be more monofractal. Finally, the *H* parameter represents the value h in which the singularity spectra has its maximum *h(D)* (Makowiec et al., 2011). The position of *h* moves to higher values when the stronger singularities are present. Highly deterministic signals can often be explained by a lower number of fractal dimensions and are characterised by smaller *W* and *H* due to a decrease in the number of singularities.

Statistical Analysis

Before any statistical analysis all variables were converted to z-scores. Those participants having z-scores larger than 3 standard deviations in three non-linear parameters or more were rejected from the analysis. In total only 1 participant in the old group was removed. Independent *t*-tests were computed to test differences between the RQA and fractal measures of the average MRI signals in both groups. Inspection of Q-Q Plots was carried out to all the measures to check

266 if the data were normally distributed. Additionally, Levene's test for equality of variances was
267 applied and, in those cases, where this assumption was violated, a *t* statistic not assuming
268 homogeneity of variance were computed on these measures. Finally, a linear regression between
269 the non-linear measures and the participants age were performed.

270 **Results**

271 ***The ZQC weighted signals***

272 Examples of the ZSE-weighted signals and their Fourier transform of both age groups are
273 shown in figure 2a-h. As it can be seen, strong cardiac signal fluctuations are resolved only in the
274 average time-series of young subjects (Figure 2a and 2c) while in older subjects the strong cardiac
275 signals are diminished (Figure 2e and 2g). The frequency spectra of the time-series (Figure 2b, 2d,
276 2f and 2h) showed the strongest cardiac frequencies for the young group, while in the older group,
277 however, the spectra show stronger harmonics, envelope waves or both, in addition to the weaker
278 cardiac frequencies. These envelope waves have a beat frequency of the (cardiac frequency)/n,
279 where n takes values of (2,3,4,6,9 ...). These results are consistent over most subjects.

280

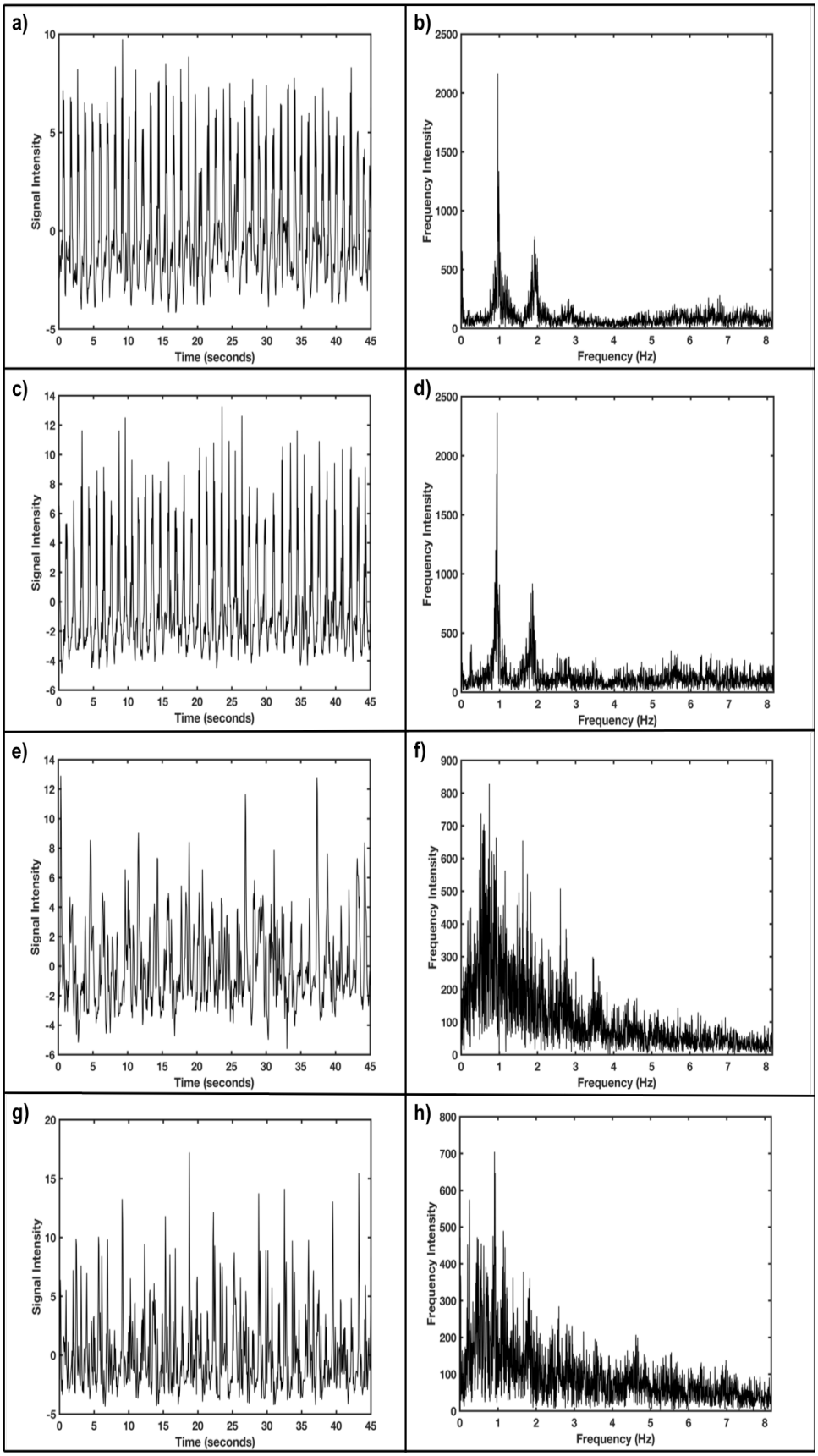

Figure 2. *Example of the time-series as well as its frequency spectra for two young (a-c and b-d) and two healthy old adults (e-g and f-h). These examples are representing the typical results in these groups.*

281

Non-linear dynamics of the ZSE weighted signal

We also tested how the non-linear dynamics varied in the ZSE weighted time-series in all participants (see Supplementary Results for the SQC results). At a group level all the RQA parameters but the DET were statistically significantly higher in the old group in comparison to the young one (see Table 1 for group averages): MeanLine ($t(57) = 2.23, p = .02; d = .58$), MaxLine ($t(57) = 2.81, p = .007; d = .73$), Ent ($t(57) = 2.62, p = .01; d = .68$), Lam ($t(57) = 3.68, p = .001; d = 0.96$) and TT ($t(57) = 4.57, p < .001; d = 1.19$) and Det ($t(57) = 1.23, p = .22; d = .32$).

Parameter	*Young*	*Old*
Det	32.16 ± 10.12	35.72 ± 11.99
MeanLine*	2.81 ±.34	3.07 ± .51
MaxLine**	99.10 ± 38.35	135.53 ± 58.63
Ent*	.77 ±.19	.92 ±.24
Lam**	35.42 ± 8.24	46.50 ± 14.00
TT*	2.24 ±.11	2.48 ± .26
W*	.15 ± .08	.27 ± .07
H*	.02 ± .01	.03 ± .01

Table 1. *Group mean averages of the RQA and MFDFA parameters extracted from the ZQC weighted time-series for the young and old groups (p < .05(*), p < .01(**), p <.001(***)).*

Likewise, the fractal properties of the ZSE weighted signal in the old group were statistically higher in W (t (57) = 5.44, $p < .001$; $d = 1.41$) and H (t (57) = 3.53, $p = .001$; $d = .92$) in comparison to the young group, suggesting a more chaotic behaviour in the old population.

Are group differences coming from movement or cognitive differences?

Since the ZSE effects are sensitive to movement, we explored the relationship between the non-linear parameters and motion quality control variables from the rs-fMRI as a proxy for potential average movement of the participant Although the information was not available for the young group, there were no significant correlations between these measures (see Table 2) or in other words, the non-linear dynamics in the old cohort were not worsened by motion.

Parameter	*QC max movement*	*QC mean movement*
Det	-.36 (.07)	.13 (.50)
MeanLine	-.10 (.60)	.00 (.97)
MaxLine	-.30 (.13)	-.01 (.95)
Ent	-.26 (.19)	.08 (.69)
Lam	-.27 (.17)	.17 (.38)
TT	-.13 (.52)	.22 (.27)
W	.06 (.77)	.02 (.92)
H	-.14 (.47)	-.06 (.77)

Table 2. *Spearman correlations between quality control movement measures from the rs-fMRI session and the non-linear parameters of the ZQC signals. In these correlations, n was equal to 27 since movement information was not available for one participant and another did not pass quality control (see section 2.5).*

Finally, we explored any possible relation to cognitive measures and tests performed during the study. CANTAB scores showed consistent negative correlations and trends (see Table 3, Figure 3) between visual memory scores (pattern recognition memory and working memory) and the RQA parameters while no correlations arose with the TNT scores. Consistently, young participants that showed higher complexity (i.e., smaller non-linear parameters) also had better cognitive scores. Altogether, there were significant changes with ageing but even more with these cognitive scores which suggest that the ZSE signal may be related to aspects of cognition.

Parameter	*Pat. Recognition Mem. (immediate recall)*	*Paired Associates Learning*	*Spat. working Mem. (strategy)*	*Pat. Recognition Mem. (delayed recall)*	*Trial A*	*Trial B*
Det	**-.31 (.01)***	.06 (.62)	-.19 (.13)	-.02 (.87)	.05 (.69)	-.02 (.87)
MeanLine	**-.33 (.009)****	-.04 (.71)	-.17 (.17)	-.13 (.31)	.00 (.98)	-.04 (.74)
MaxLine	**-.34 (.008)****	-.18 (.16)	**-.26 (.04)***	-.19 (.12)	-.00 (.96)	-.02 (.86)
Ent	**-.33 (.009)****	.06 (.65)	-.21 (.10)	-.12 (.33)	.09 (.49)	-.04 (.76)
Lam	**-.29 (.02)***	.03 (.78)	**-.34 (.008)****	-.09 (.48)	-.04 (.72)	-.05 (.68)
TT	-.25 (.05)+	-.08 (.51)	**-.29 (.02)***	-.18 (.15)	.01 (.90)	-.07 (.57)
W	-.18 (.14)	-.04 (.71)	-.13 (.29)	-.17 (.17)	.25 (.06)+	.13 (.31)
H	-.24 (.06)+	.04 (.75)	-.22 (.10)	-.09 (.48)	.00 (.95)	.07 (.60)

Table 3. Spearman correlations between the non-linear parameters of the ZQC signals and the CANTAB and TNT scores. In these correlations, n varies between 59 (CANTAB scores) and 55 (TNT scores) since one participant did not pass quality control (see section 2.5) and the measures were not available to all of them. p-values are in parenthesis (trend (+) p <.05(*) and p <.01(**)).

Discussion

In this paper, we have analysed if the dynamical complexity of ZSE fluctuations in the brain tissue varies with age. While comparing two populations, we presented qualitative evidence that the strong cardiac constant fluctuations are more likely resolved for the younger subjects while for the older ones, the strong cardiac effect is diminished. Non-linear analyses confirmed this effect and showed quantitative differences between both age groups, which were related to variations in complexity and chaos of the measured signals. Particularly, the higher complexity of ZSE weighted signal was related to better cognitive performance in some of the CANTAB scales, which was not correlated to age. Altogether, this may suggest that the ZSE fluctuations may be sensitive to ageing, cognition or even differences in wakefulness.

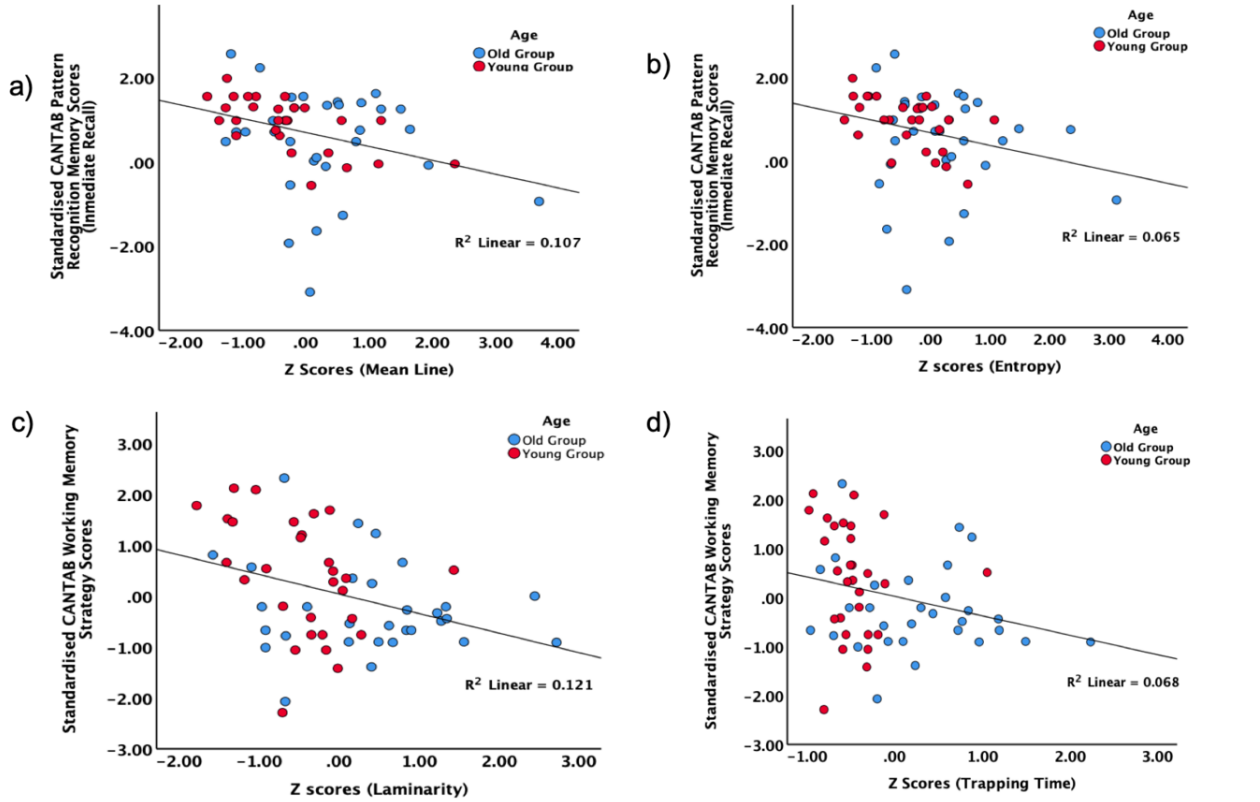

Figure 3. *Examples of linear regressions between mean line (a) and entropy(b), and Standardised CANTAB Pattern Recognition Memory Scores (Inmediate Recall), and between Laminarity (c) and Trapping Time (d), and standardised CANTAB working memory strategy scores.*

316 The changes in the ZSE weighted signal were manifold, varying in shape, amplitude and
317 frequency (see Figure 2). In particular, older participants possessed a higher number of frequencies
318 as well as a decrease in the size and number of the cardiac bursts. On the other hand, the younger
319 group was characterised by roughly constant bursts and clear cardiac frequencies with almost no
320 harmonics. Initially, one may think that differences between both groups can be due to old
321 participants moving more inside the scanner. In fact, López Pérez and Kerskens (2019) reported
322 that during hyperventilation inside the scanner the ZSE effect entirely vanished due to increased
323 movement. Although the information was not available for the young group, motion quality control
324 variables from an fMRI study within the same session did not correlate with any of the non-linear
325 parameters (see Table 2). Thus, we can conclude that the dynamics in the older cohort were not
326 worsened by motion. Regardless of this, future studies using the sequence should try to minimise

the effect of movement during the data acquisition (e.g., adding extra cushions to hold the head) which might help improve the intensity of the quantum effect (López Pérez & Kerskens, 2019).

A second possibility is that the ZSE signal declines with changes in cognition or age. To check that, we first quantified the apparent differences between both groups using non-linear time-series analyses to determine changes in the dynamics of the MRI signals. First, we applied Recurrence Quantification Analysis (RQA), which was proven to be sensitive to small changes in the system dynamics and a powerful discriminatory tool to detect significant differences between both age groups (see Supplementary files for further discrimination analysis between both groups based on these measures). All the RQA measures (see Table 1 and Supplementary Table 1) were lower in the young group in comparison to the older group in both types of MRI signals, suggesting differences in the complexity of the underlying signal dynamics in both populations. Second, we applied fractal analysis to study the fractal scaling properties and long-range correlations of the signals. We showed an increase in the number of singularities with age, which is characterised by an increase in the width and position of the spectral maxima (Ihlen, 2012; Dick & Svyatogor, 2012). These differences were supported by the RQA entropy which denotes the Shannon entropy of the histogram of the lengths of diagonal segments and thus indicates the complexity of the deterministic structure of the system (Dos Santos et al., 2014). This increase in the chaoticity of the signal is only visible when the quantum effects are measured since no differences were found between the fractal parameters in the control condition (see Supplementary Table 1). Additionally, exploratory analyses showed an incremental tendency with age (see Supplementary Figures 1 and 2), but these results need to be replicated with an independent sample where a whole range of ages gets included.

The ZSE declines with age but does it relate to cognition? Our results are in line with recent studies indicating that higher complexity in a system is a feature of healthy dynamics (Dos Santos et al., 2014) or higher degree of functional specialisation and integration in brain dynamics (Ho et al., 2017) and that this complexity declines with disease and age (e.g., Manor & Lipsitz, 2013). In fact,

we observed some significant negative correlations between CANTAB scores, and RQA measures (see Table 3), were lower scores (i.e., higher complexity) were related to better cognitive scores. Particularly significant were the relations with pattern recognition memory and working memory subscales, suggesting a link between the ZSE signal and short-term memory abilities. A potential explanation why the ZSE signal was correlated to pattern recognition memory and spatial working memory is that the acquisition slice was roughly located in parietal and posterior cingulate regions and these are areas associated with these cognitive domains (e.g., Guttmann et al., 1998; Gunning-Dixon & Raz, 2003). Paired associates learning, however, is a hippocampus-based task (Provyn, Sliwinski & Howard, 2007) and therefore one would not expect to find a correlation with the measured signal. Besides, fMRI studies have shown that healthy old adults present higher activity levels in some brain regions during the performance of cognitive tasks and these changes coexist with disrupted connectivity (for a review see Sala-Llonch, Bartrés-Faz & Junqué, 2015). However, to the best of our knowledge, there are not fMRI-based signals that are able to predict these CANTAB scores consistently. This is especially surprising since the ZSE signal represents the average over the imaging slice and is a very rough and functional measurement. More importantly, the pattern recognition memory and working memory subscales that were strongly correlated with the non-linear parameters did not correlate with age (see Supplementary Table 3), which emphasises the sensitivity of the ZSE signal to cognitive changes. Thus, we believe that these fluctuations, which may originate from exotic phase transitions over the entire brain (Kerskens, 2020), could be a global physiological effect essential for understanding cognition and consciousness with clinical relevance for all neurovascular diseases.

However, several limitations arise in this study. First, the acquisition protocol applied to obtain the ZSE weighted signal required fast repetition times, which limits the number of imaging slices to just one. The use of one imaging slice complicates the study of particular areas and it could induce variability in the results across all the participants even when the position of the imaging slice is carefully planned. As a consequence, different slices should be acquired to study

a larger region and improve the comparison between groups. Some approaches could be used to overcome this limitation. For example, next-generation MRI systems can acquire three or more imaging slabs by means of Multi-band excitation (Feinberg et al., 2010) with the same time resolution. A second improvement can be achieved with the increase in the number of channels in the receiver coil, which allow the acquisition of data with shorter repetition times and better signal to noise ratio. Future research should focus on expanding the sequence protocol to be able to cover larger brain areas that would allow the use of the sequence in a wide range of studies. Secondly, differences in wakefulness among participants and between groups may have impacted the results. Lopez Pérez and Kerskens (2019) showed that participants that fell asleep during testing showed no significant ZSE signal. Despite the fact that the radiographer was checking that all volunteers were awake before the data acquisition, under these conditions (i.e., testing in a supine position inside a dark room with no specific instructions but to remain still) participants in the older group are more likely to feel sleepy, thus potentially affecting their wakefulness. Finally, the group sizes in this study were small and the results need to be considered preliminary. Further research is needed to confirm these findings.

Conclusions

We have provided further evidence that heartbeat related ZSE signals in the brain are related to consciousness, cognition and ageing. We showed qualitatively and quantitatively that these fluctuations worsen with age and that their decline is related to a decrease in the complexity of the signal time series. Consistent with the idea that higher complexity is related to healthier dynamics, our signal contrast showed higher complexity in the younger population. Altogether, the ZSE signal is a promising biomarker that needs to be tested in larger and more diverse populations with clinical relevance for all neurovascular diseases.

Conflict of Interest

The authors have declared no conflict of interest

References

1. Al, E., Iliopoulos, F., Forschack, N., Nierhaus, T., & Grund, M. (2020). Heart – brain interactions shape somatosensory perception and evoked potentials. *ELife*, *201915629*, 1–10. https://doi.org/10.1073/pnas.1915629117

2. Alderson, T., Kehoe, E., Maguire, L., Farrell, D., Lawlor, B., Kenny, R. A., … Coyle, D. (2017). Disrupted thalamus white matter anatomy and posterior default mode network effective connectivity in amnestic mild cognitive impairment. Frontiers in Aging Neuroscience, 9(NOV). https://doi.org/10.3389/fnagi.2017.00370

3. Allen, J. S., Bruss, J., Brown, C. K., & Damasio, H. (2005). Normal neuroanatomical variation due to age: The major lobes and a parcellation of the temporal region. Neurobiology of Aging, 26(9), 1245–1260. https://doi.org/10.1016/j.neurobiolaging.2005.05.023

4. Archer, J. A., Lee, A., Qiu, A., & Chen, S. H. A. (2018). Working memory, age and education: A lifespan fMRI study. *PLoS ONE*, *13*(3). https://doi.org/10.1371/journal.pone.0194878

5. Arnett, J. A., & Labovitz, S. S. (1995). Effect of physical layout in performance of the Trail Making Test. *Psychological Assessment*, *7*(2), 220–221. https://doi.org/10.1037/1040-3590.7.2.220

6. Balota, D.A., Dolan P.O. & Duchek J.M. (2000). In: The Oxford Handbook of Memory. Tulving E., Craik F., editors. Oxford University Press; pp. 395–410.

7. Bosl, W. J., Loddenkemper, T., & Nelson, C. A. (2017). Non-linear EEG biomarker profiles for autism and absence epilepsy. *Neuropsychiatric Electrophysiology*, *3*(1). https://doi.org/10.1186/s40810-017-0023-x

8. Carstensen LL, et al. (2011) Emotional experience improves with age: evidence based on over 10 years of experience sampling. Psychol Aging ;26:21–33.

9. Censi F., Calcagnini G., Cerutti S. (2015) Dynamic Coupling Between Respiratory and Cardiovascular System. In: Webber, Jr. C., Marwan N. (eds) Recurrence Quantification Analysis. Understanding Complex Systems. Springer, Cham.

10. Craik, F.I.M. & Bosman, E.A. (1992) In: Gerontechnology: Proceedings of the First International Conference on Technology and Aging. Bouma H, Graafmans J, editors. IOS Press; pp. 79–92.

11. Dick, O. E., & Svyatogor, I. A. (2012). Potentialities of the wavelet and multifractal techniques to evaluate changes in the functional state of the human brain. *Neurocomputing*, *82*, 207–215. https://doi.org/10.1016/j.neucom.2011.11.013

12. Dos Santos, L., Barroso, J. J., De Godoy, M. F., Macau, E. E. N., & Freitas, U. S. (2014). Recurrence quantification analysis as a tool for discrimination among different dynamics classes: The heart rate variability associated to different age groups. In *Springer Proceedings in Mathematics and Statistics* (Vol. 103, pp. 125–136). Springer New York LLC. https://doi.org/10.1007/978-3-319-09531-8_8

13. Engel, G. S., Calhoun, T. R., Read, E. L., Ahn, T. K., Mančal, T., Cheng, Y. C., … Fleming, G. R. (2007). Evidence for wavelike energy transfer through quantum coherence in photosynthetic systems. Nature, 446(7137), 782–786. https://doi.org/10.1038/nature05678

448 14. Feinberg, D. A., Moeller, S., Smith, S. M., Auerbach, E., Ramanna, S., Glasser, M. F., …
449 Yacoub, E. (2010). Multiplexed echo planar imaging for sub-second whole brain fmri and
450 fast diffusion imaging. *PLoS ONE*, *5*(12). https://doi.org/10.1371/journal.pone.0015710

451 15. Gilligan, T. M., Sibilia, F., Farrell, D., Lyons, D., Kennelly, S. P., & Bokde, A. L. W.
452 (2019). No relationship between fornix and cingulum degradation and within-network
453 decreases in functional connectivity in prodromal Alzheimer's disease. PLoS ONE, 14(10).
454 https://doi.org/10.1371/journal.pone.0222977

455 16. Gómez, C., & Hornero, R. (2010). Entropy and Complexity Analyses in Alzheimer's
456 Disease: An MEG Study. *The Open Biomedical Engineering Journal*, *4*(1), 223–235.
457 https://doi.org/10.2174/1874120701004010223

458 17. Goyal, M. S., Vlassenko, A. G., Blazey, T. M., Su, Y., Couture, L. E., Durbin, T. J., …
459 Raichle, M. E. (2017). Loss of Brain Aerobic Glycolysis in Normal Human Aging. Cell
460 Metabolism, 26(2), 353-360.e3. https://doi.org/10.1016/j.cmet.2017.07.010

461 18. Grady, C. L. (2008). Cognitive neuroscience of aging. *Annals of the New York Academy of*
462 *Sciences*. Blackwell Publishing Inc. https://doi.org/10.1196/annals.1440.009

463 19. Grady, C. (2012). Trends in Neurocognitive Aging. *Nature Reviews. Neuroscience*, *13*(7),
464 491–505. https://doi.org/10.1038/nrn3256

465 20. Grady, C. L., McIntosh, A. R., Horwitz, B., Maisog, J. M., Ungerleider, L. G., Mentis, M.
466 J., … Haxby, J. V. (1995). Age-related reductions in human recognition memory due to
467 impaired encoding. *Science*, *269*(5221), 218–221.
468 https://doi.org/10.1126/science.7618082

469 21. Grady, C. L., Maisog, J. M., Horwitz, B., Ungerleider, L. G., Mentis, M. J., Salerno, J. A.,
470 … Haxby, J. V. (1994). Age-related changes in cortical blood flow activation during visual

processing of faces and location. *Journal of Neuroscience*, *14*(3 II), 1450–1462. https://doi.org/10.1523/jneurosci.14-03-01450.1994

22. Gunning-Dixon, F. M., & Raz, N. (2003). Neuroanatomical correlates of selected executive functions in middle-aged and older adults: a prospective MRI study. Neuropsychologia, 41(14), 1929-1941.

23. Guttmann, C. R., Jolesz, F. A., Kikinis, R., Killiany, R. J., Moss, M. B., Sandor, T., & Albert, M. S. (1998). White matter changes with normal aging. Neurology, 50(4), 972-978.

24. Hirata, Y., & Aihara, K. (2010). Devaney's chaos on recurrence plots. *Physical Review E - Statistical, Non-linear, and Soft Matter Physics*, *82*(3). https://doi.org/10.1103/PhysRevE.82.036209

25. Ho, P.S, Lin, C., Chen, G. Y., Liu, H. L., Huang, C.M., Lee, T.M., Lee, S.H., & Wu, S.C. (2017). Complexity analysis of resting state fMRI signals in depressive patients. *Conference proceedings : ... Annual International Conference of the IEEE Engineering in Medicine and Biology Society. IEEE Engineering in Medicine and Biology Society. Annual Conference*, *2017*, 3190–3193. https://doi.org/10.1109/EMBC.2017.8037535

26. Huelga, S. F., & Plenio, M. B. (2013, July). Vibrations, quanta and biology. Contemporary Physics. https://doi.org/10.1080/00405000.2013.829687

27. Ihlen, E. A. F. (2012). Introduction to multifractal detrended fluctuation analysis in Matlab. *Frontiers in Physiology*, *3 JUN*. https://doi.org/10.3389/fphys.2012.00141

28. Jedlicka, P. (2017). Revisiting the quantum brain hypothesis: Toward quantum (neuro)biology? *Frontiers in Molecular Neuroscience*, *10*. https://doi.org/10.3389/fnmol.2017.00366

494 29. Kehoe, E. G., Farrell, D., Metzler-Baddeley, C., Lawlor, B. A., Kenny, R. A., Lyons, D.,
495 … Bokde, A. L. (2015). Fornix white matter is correlated with resting-state functional
496 connectivity of the thalamus and hippocampus in healthy aging but not in mild cognitive
497 impairment - A preliminary study. *Frontiers in Aging Neuroscience*, *7*(FEB).
498 https://doi.org/10.3389/fnagi.2015.00010

499 30. Kennel, M. B., Brown, R., & Abarbanel, H. D. I. (1992). Determining embedding
500 dimension for phase-space reconstruction using a geometrical construction. *Physical*
501 *Review A*, *45*(6), 3403–3411. https://doi.org/10.1103/PhysRevA.45.3403

502 31. Kerskens, C.M. Are Qualia Reducible, Physical Entities? Preprints 2020, 2020030459
503 doi:10.20944/preprints202003.0459.v1

504 32. Laver, G.D. (2009). Adult aging effects on semantic and episodic priming in word
505 recognition. Psychol Aging ;24:28–39.

506 33. Liu, P., Hebrank, A. C., Rodrigue, K. M., Kennedy, K. M., Section, J., Park, D. C., & Lu,
507 H. (2013). Age-related differences in memory-encoding fMRI responses after accounting
508 for decline in vascular reactivity. *NeuroImage*, *78*, 415–425.
509 https://doi.org/10.1016/j.neuroimage.2013.04.053

510 34. Lopes, R., & Betrouni, N. (2009). Fractal and multifractal analysis: A review. *Medical*
511 *Image Analysis*, *13*(4), 634–649. https://doi.org/10.1016/j.media.2009.05.003

512 35. López Pérez, D. & Kerskens, C. M. (2019). Cardiac-evoked long-range quantum
513 entanglement in the conscious brain. Biorxiv. https://doi.org/10.1101/219931

514 36. Ma, Q., Ning, X., Wang, J., & Bian, C. (2006). A new measure to characterize
515 multifractality of sleep electroencephalogram. *Chinese Science Bulletin*, *51*(24), 3059–
516 3064. https://doi.org/10.1007/s11434-006-2213-y

517 37. Makowiec, D., Rynkiewicz, A., Gaaska, R., Wdowczyk-Szulc, J., & Arczyńska-
518 Buchowiecka, M. (2011). Reading multifractal spectra: Aging by multifractal analysis of
519 heart rate. *EPL*, *94*(6). https://doi.org/10.1209/0295-5075/94/68005

520 38. Manor, B., & Lipsitz, L. A. (2013). Physiologic complexity and aging: Implications for
521 physical function and rehabilitation. *Progress in Neuro-Psychopharmacology and*
522 *Biological Psychiatry*, *45*, 287–293. https://doi.org/10.1016/j.pnpbp.2012.08.020

523 39. Marwan, N., Wessel, N., Meyerfeldt, U., Schirdewan, A., & Kurths, J. (2002). Recurrence-
524 plot-based measures of complexity and their application to heart-rate-variability
525 data. *Physical Review E - Statistical Physics, Plasmas, Fluids, and Related*
526 *Interdisciplinary Topics*, *66*(2). https://doi.org/10.1103/PhysRevE.66.026702

527 40. Marwan, N., Carmen Romano, M., Thiel, M., & Kurths, J. (2007, January). Recurrence
528 plots for the analysis of complex systems. *Physics Reports*.
529 https://doi.org/10.1016/j.physrep.2006.11.001

530 41. Marwan, N., & Webber, C. L. (2015). Mathematical and computational foundations of
531 recurrence quantifications. *Understanding Complex Systems*, 3–43.
532 https://doi.org/10.1007/978-3-319-07155-8-1

533 42. Montoya, P., Schandry, R., & Müller, A. (1993). Heartbeat evoked potentials (HEP):
534 topography and influence of cardiac awareness and focus of
535 attention. *Electroencephalography and Clinical Neurophysiology/ Evoked*
536 *Potentials*, *88*(3), 163–172. https://doi.org/10.1016/0168-5597(93)90001-6

537 43. Ogawa, S., Lee, T. M., Kay, A. R., & Tank, D. W. (1990). Brain magnetic resonance
538 imaging with contrast dependent on blood oxygenation. *Proceedings of the National*
539 *Academy of Sciences of the United States of America*, *87*(24), 9868–9872.
540 https://doi.org/10.1073/pnas.87.24.9868

541 44. Peng, C. K., Costa, M., & Goldberger, A. L. (2009). Adaptive data analysis of complex
542 fluctuations in physiologic time-series. *Advances in Adaptive Data Analysis*, *1*(1), 61–70.
543 https://doi.org/10.1142/S1793536909000035

544 45. Pignat, J. M., Koval, O., Van De Ville, D., Voloshynovskiy, S., Michel, C., & Pun, T.
545 (2013). The impact of denoising on independent component analysis of functional
546 magnetic resonance imaging data. *Journal of Neuroscience Methods*, *213*(1), 105–122.
547 https://doi.org/10.1016/j.jneumeth.2012.10.011

548 46. Pereda, E., Gamundi, A., Rial, R., & González, J. (1998). Non-linear behaviour of human
549 EEG: Fractal exponent versus correlation dimension in awake and sleep
550 stages. *Neuroscience Letters*, *250*(2), 91–94. https://doi.org/10.1016/S0304-
551 3940(98)00435-2

552 47. Provyn, J. P., Sliwinski, M. J., & Howard, M. W. (2007). Effects of Age on Contextually
553 Mediated Associations in Paired Associate Learning. Psychology and Aging, 22(4), 846–
554 857. https://doi.org/10.1037/0882-7974.22.4.846

555 48. Reitan, R. M. (1958). Validity of the Trail Making Test as an Indicator of Organic Brain
556 Damage. *Perceptual and Motor Skills*, *8*(3), 271–276.
557 https://doi.org/10.2466/pms.1958.8.3.271

558 49. Robbins, T. W., James, M., Owen, A. M., Sahakian, B. J., McInnes, L., & Rabbitt, P.
559 (1994). Cambridge neuropsychological test automated battery (CANTAB): A factor
560 analytic study of a large sample of normal elderly volunteers. *Dementia*.
561 https://doi.org/10.1159/000106735

562 50. Roulston, M. S. (1999). Estimating the errors on measured entropy and mutual
563 information. *Physica D: Non-linear Phenomena*, *125*(3–4), 285–294.
564 https://doi.org/10.1016/S0167-2789(98)00269-3

565 51. Sala-Llonch, R., Bartrés-Faz, D., & Junqué, C. (2015). Reorganization of brain networks
566 in aging: a review of functional connectivity studies. *Frontiers in Psychology*, *6*.
567 https://doi.org/10.3389/fpsyg.2015.00663

568 52. Salat, D. H., Buckner, R. L., Snyder, A. Z., Greve, D. N., Desikan, R. S. R., Busa, E.,
569 Morris, J. C. Dale, A. M. & Fischl, B. (2004) Thinning of the Cerebral Cortex in Aging,
570 *Cerebral Cortex*, Volume 14, Issue 7, July, Pages 721–730,
571 https://doi.org/10.1093/cercor/bhh032

572 53. Salthouse, T.A. (1996). The processing-speed theory of adult age differences in cognition.
573 Psychol Rev. ;103:403–428.

574 54. Scholes, G. D., Fleming, G. R., Chen, L. X., Aspuru-Guzik, A., Buchleitner, A., Coker, D.
575 F., … Zhu, X. (2017, March 29). Using coherence to enhance function in chemical and
576 biophysical systems. *Nature*. Nature Publishing Group.
577 https://doi.org/10.1038/nature21425

578 55. Thiel, M., Romano, M. C., Kurths, J., Meucci, R., Allaria, E., & Arecchi, F. T. (2002).
579 Influence of observational noise on the recurrence quantification analysis. *Physica D: Non-*
580 *linear Phenomena*, *171*(3), 138–152. https://doi.org/10.1016/S0167-2789(02)00586-9

581 56. Tsvetanov, K.A., Henson, R.N., & Rowe, J.B. (2019). Separating vascular and neuronal
582 effects of age on fMRI BOLD signals. arXiv: Neurons and Cognition.

583 57. Wessel, N., Marwan, N., Schirdewan, A., & Kurths, J. (2003). Beat-to-beat complexity
584 analysis before the onset of ventricular tachycardia. In *Computers in Cardiology* (Vol. 30,
585 pp. 477–480). https://doi.org/10.1109/cic.2003.1291196

586 58. Zbilut, J. P., & Webber, C. L. (1992). Embeddings and delays as derived from
587 quantification of recurrence plots. *Physics Letters A*, *171*(3–4), 199–203.
588 https://doi.org/10.1016/0375-9601(92)90426-M